Evaluation of Dynamic Scheduling for Data Collection in Medical Application Using Firefly Synchronization Algorithm

Norhafizah Muhammad(✉) and Tiong Hoo Lim

Universiti Teknologi Brunei, Gadong, Brunei
{norhafizah.muhammad,lim.tiong.hoo}@utb.edu.bn

Abstract. This paper proposed a dynamic data transmission scheduling algorithm based on the way a group of firefly communicating with one another. The proposed algorithm will be compared again with a random transmission approach. To evaluate the performance of the algorithms, different numbers of nodes in the networks will be evaluated. The results from the hardware experiments have shown that the firefly algorithm can schedule the transmission of data packet with high delivery rate for a small network. However, as the number of nodes increases, the packet delivery rate decreases. The proposed algorithm can also increase the lifespan of the battery as the nodes will be operating in the sleep mode and will only be awake during the sychronization period for data transmission.

Keywords: Firefly algorithm · Bio-inspired · Sychronization · Transmission scheduling · Health monitoring

1 Introduction

In the vast development of the wireless body sensor networks, one of the applications is the healthcare monitoring system. The monitoring system will be able to sense and alert any abnormality of the patient's health to the personal care, such as the caretaker or emergency center. The sensed data will be collected from the devices that are on or implanted in the patient's body. It is important to collect and transmit the sensed data in synchronous, real-time and continuous manner. Data synchronicity is defined as the ability to collect and transmit sensing data across biosensor networks in an orderly time sequential manner. Time synchronization is important during the transmission of data in time-sensitive applications such as medical health. The data need to be received according to the order of the data are used for diagnostic in an Artificial Intelligence based on the medical application. Djenouri et al. [9] stated that the node should be synchronized to correlate the different reports of information. Zong et al. [4] mentioned the applications of time synchronization can be collaborated, coordinated and localized the position of the nodes. The authors also highlighted that

H. Gao et al. (Eds.): ChinaCom 2020, LNICST 352, pp. 142–160, 2021.
https://doi.org/10.1007/978-3-030-67720-6_10

the sensor nodes are dedicated in cooperating and monitoring the physical or environmental variables, which requires the precise timing among the nodes.

Fixed time synchronization algorithm has been used in the MAC layer to ensure that data can be collected and transmitted reliable at a predetermined interval. In fixed time synchronization, the transmission interval allocated to individual node is equally divided among a set of nodes within a time period. Each node will need to transmit at the assigned interval to avoid packet collisions using time division approaches. However, fixed time synchronization approach is not suitable for medical application as the sensing data needs to be transmitted at any time when a critical event is detected. The default CSMA/CA transmission protocol at the MAC layer is prone to collision when the number of biosensor nodes increases. Hence, there is a need to apply bio-inspired synchronization algorithm at the application layer to ensure that the patient physiological data can be received promptly and reliably.

Bio-inspired algorithms are based on the behaviour of a large biological swarms that is dynamic in nature. These algorithms are shown to tolerate to failure and can dynamically recover from failures. In this paper, a firefly-inspired scheduling algorithm for data transmission is proposed and implemented at the application layer to improve the packet delivery rate while reducing the energy consumption in the nodes through duty cycling. By synchronizing the biosensor to transmit at the same time, it can improve the energy efficiency of each nodes as all the node can off its radio. All the biosensor nodes can wake up at the same time for a short period of time, sample their sensors and transmit immediately to the base station or relay the data along the routing path to the base station without interfering with other nodes [1]. The transmission will be coordinated and interleaved with the awake period. Once all the nodes have transmitted, each node will switch from transmitting mode to sleep/listening mode to reduce energy consumption.

2 Related Works

Bio-inspired synchronicity is a simple model based on the natural phenomenon in the world, for examples colony of ants complete the difficult task, school of fish navigate the sea and swarm of fireflies flashing in a perfect unison [1]. There are related works had been done by using the bio-inspired approach in Wireless Body Sensor Networks. By adapting and implementing a biological inspired systems into a network of nodes, individual node in the network can behave and inherit the adaptive and fault tolerance of the animals or insects. In [2,3], the proposed system can adapt any types of environments, resistance in any internal or external failures, evolve and learn new conditions, and self-organized in a fully distributed and efficient collaboration manners.

Mirollow and Strogatz [7] proposed a mathematical model based on a pulse-coupled oscillator to mimic the behavior of a firefly to synchronize the clock operating in a set of sensor nodes. An individual node will broadcast a pulse periodically to its neighbour. When the neighboring node within its transmission

range received the transmitted pulse, it will adjust its internal clock to the time its received the firing pulse or oscillators and respond by sending its own pulse. This process will repeat until all the pulse received are synchronized. In [1] stated that the synchronicity can be used to coordinate the sampling across multiple nodes for the important applications that need a high data rate. However, Zong et al. [4] highlight that the pulse-coupled approach can only achieve synchronization if the internal dynamic oscillators are identical and no coupling delay during the packet exchange among the oscillators. When anode sends out a fire message at time, t_{fire}, the neighboring nodes will not received the message immediately. As a result, those nodes will only respond after $t_{fire} + \alpha$ where α is an unknown propagation delay. An et al. [8] implemented a linear pulsed- coupled oscillator model with linear dynamic with different coupling strength to avoid synchronization error when there is an interruption in the network.

In Werner-Allen et al. [4], the authors developed the Reach-back Firefly Algorithm (RFA) that uses previous transmission information to adjust the future firing phase of the sensor nodes. The authors highlighted that the RFA can overcome the timestamping messages by staggering the messages. Movassaghi et al. [6] found out that the protocol achieved stability and robust to nodes leaving or joining the networks. The system was able to self-adjust at the time of transmissions. However, the authors did not consider the stringent battery and infeasibility memory of the nodes in WBSN [6].

Adhikary et al. [7] designed a Particle Swarm Intelligent Optimzation based on flocking bird to improve the scalability of the system network. The authors showed that by optimizing the transmission power and allocating the bandwidth, it can maximize the system throughput and mitigate the inter WBSN interference. The algorithm was evaluated using MATLAB. The results have shown that the numbers of data loss increase with the transmission rate.

3 Bio-inspired Firefly Scheduling Algorithm for Data Transmission

The firefly inspired synchronization was first introduced by the Mirollo and Strogratz in 1990 [4]. According to Mirollo et al., the M&S model is a synchronization technique based on the pulse-coupled oscillation where the node will only needs to observe the firing events from the neighbor [7]. This model described that the phase node has a function of *f(t)*, which increases to a period time $t = T$ as shown in Fig. 1. When *f(t)* reaches the threshold, the node will fire and returns to zero.

$$t^{''} = f^{-1}(f(t^{'}) + \epsilon) \tag{1}$$

Figure 1 shows when a node fires, the neighbor's node will respond to the firing event and consequently adjusting its own phase forward. The new phase can be obtained by using Eq. 1, where $t^{''}$ is the new internal time and ϵ is the coupling parameter.

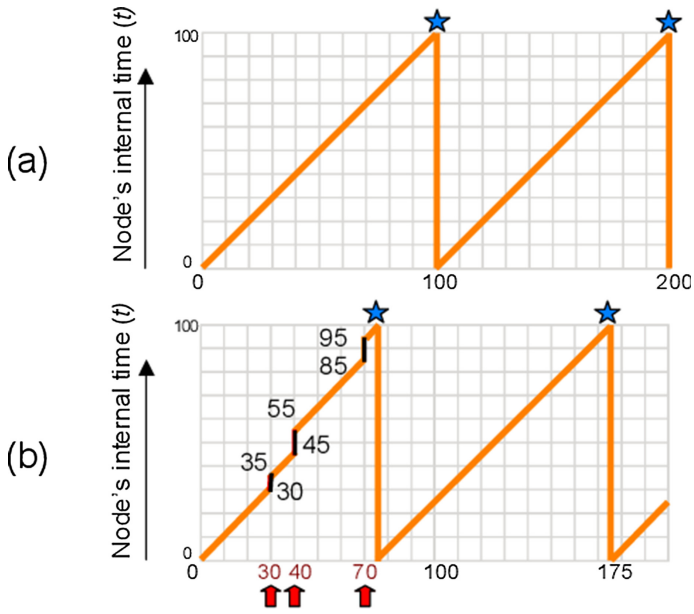

Fig. 1. Adaptive Transmission Scheduling Algorithm (a) Node fires at a time period T. (b) Node responds to neighbors firing [59]

In the proposed algorithm, Eq. 1 is modified to reduce the time of the next firing. This will allow the node to shift its next firing timing closer to its neighbour without interfering. This can be achieved by modifying the epsilon parameter using the Eq. 2.

$$f(x) = f^{-1}(f(t^{'}) - \epsilon) \tag{2}$$

The value of ϵ is determined by 3.

$$\epsilon = (t^{''} - t^{'}) - \alpha \tag{3}$$

where α is a synchronization constant. This will reduce the transmission period for all the nodes in the networks. This mathematical model shows that when a node fired, the neighbors will adjust their position by using the equation (1) above. For example, node B will observes the neighbor's time of firing. Node B will adjust the time by moving forward. This process will proceed for all nodes and this will shorten the time to broadcast the data. Therefore, when all of the nodes broadcasted or fired its information, the nodes will go to sleep until the external reaches the period of time, T.

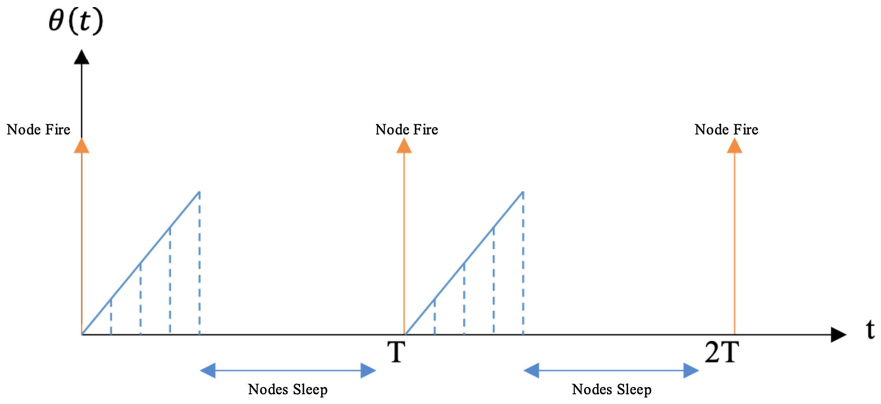

Fig. 2. The Dynamic Data Scheduling Algorithm.

4 Experimental Setup

The setup of the sensor nodes will be deployed similar to the application in the healthcare monitoring systems shown in Fig. 3. The sensor nodes or bio sensors can be connected on or implanted into the human body can be represented as the electrocardiogram (ECG), electroencephalography (EEG), pulse rate, blood pressure, body temperature and so on. The WBAN of the Fig. 3 will be operating in a star topology configuration, where all the sensor nodes are connected to the hub or gateway by using single hop communications.

Synchronization algorithm was installed and evaluated on the TelosB and XM1000 running TinyOS. A TelosB node will be used as a monitoring base station to collect the synchronization statistics and monitor the scheduling of the data transmission. XM1000 mote will be used as the individual sensor nodes that will collect environmental information to be transmitted within a clock cycle, T_{Cycle}. A 32 kHz crystal clock oscillator was used for local time. Each of the sensor nodes will have a unique id.

Different numbers of 5, 10, 15 XM1000 motes were used to evaluate the scalability of the proposed algorithms. The deployment of 5 nodes are shown in Fig. 4. A laptop will be connected to the monitoring node to store and display the statistics collected. The synchronization process will begin when the first node starts to fire. The rest of the sensor nodes receiving the message will adjust its transmission period and transmit its own messages. This process will continue until the experiment ends.

Two experiments are conducted. One experiment will be run without the firefly scheduling algorithm and will be used to compare the stability of the synchronization algorithm and the Packet Delivery Rate.

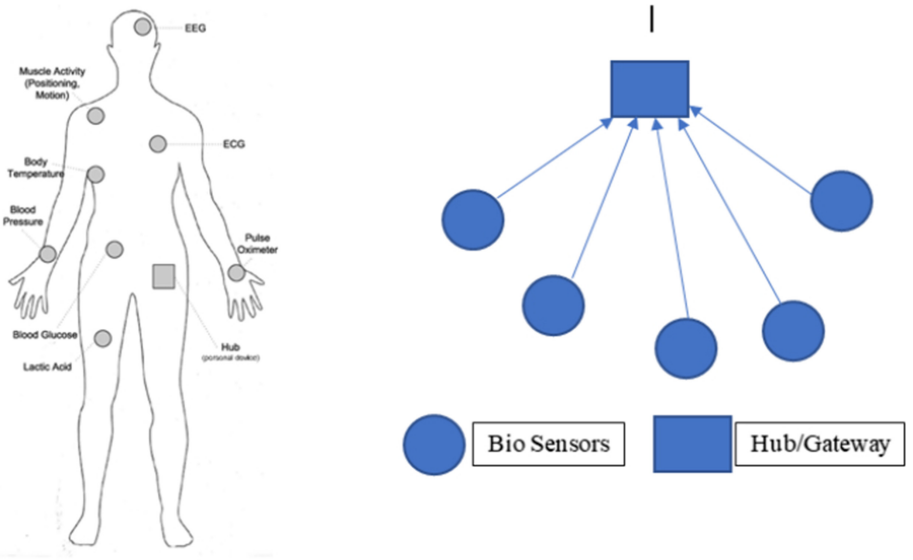

Fig. 3. The Experimental Setup for 5 XM1000 sensing nodes and 1 TelosB monitoring node.

Fig. 4. The hardware used for the experiment with one telosB mote connected to the notebook for data collection

5 Results

In this section, the performance analysis of the dynamic Scheduling for data collection based on the firefly synchronization algorithms applied in Medical Application is compare against normal CSMA/CA random transmission. Two metrics have been used to compare the performance namely the sequencing order of the packet received and the Packet Delivery Rate as the number of nodes increases.

5.1 Sequencing of Packet Delivered for 5 Nodes

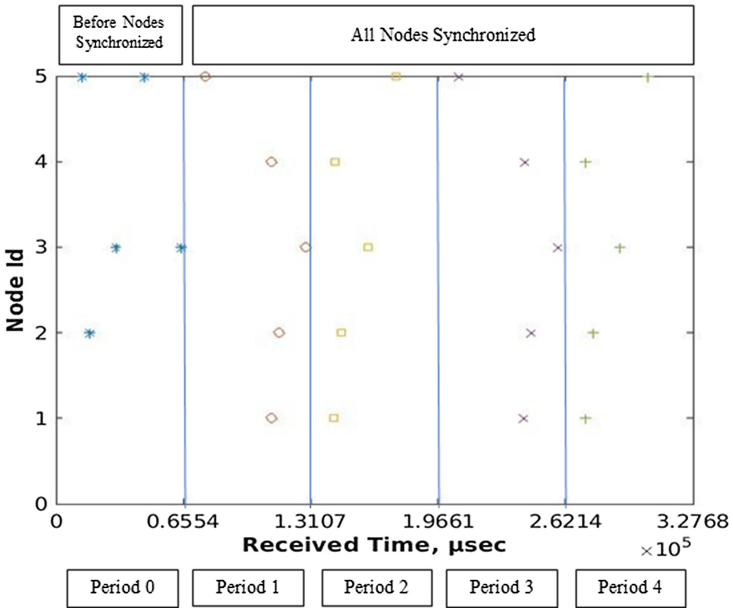

Fig. 5. The order of packet received by the basestation from 5 nodes using the random transmission scheduling algorithm for Synchronity

Figure 5 shows the process of the synchronizing of the nodes. During the synchronization process in period 0, all nodes were collected and identified on how many nodes involved. During this period, all of the sensor nodes will be equally divided and assigned time slot for transmission. By observation from Fig. 5 below shows that in period 1 to period 4, the sensor nodes shows that biosensors were in a synchronized. But there were also one or two nodes were not in synchronized, for node 2 and node 3 of periods 2 and 4 respectively. This means that there were delay in transmitting and broadcasting of the data. In period 4, Node 5 also shows there was delay in transmitting to the basestation. The cause of this delay could be either because of signal interference or traffic during the transmission.

While in Fig. 6 below shows during the synchronization process in period 0, all nodes were collected and identified on how many nodes involved. During this period, all of the sensor nodes will be equally divided and assigned time slot for transmission. By observation it shows that in period 1 to period 4, the sensor nodes showed the data transmitted in synchronized. But there were also one or two nodes were not in synchronized, for node 2 and node 3 of periods 2 and 4 respectively. This means that there were delay in transmitting and broadcasting of the data. In period 4, Node 5 also shows there was delay in transmitting to the basestation. The cause of this delay could be either because of signal interference or traffic during the transmission.

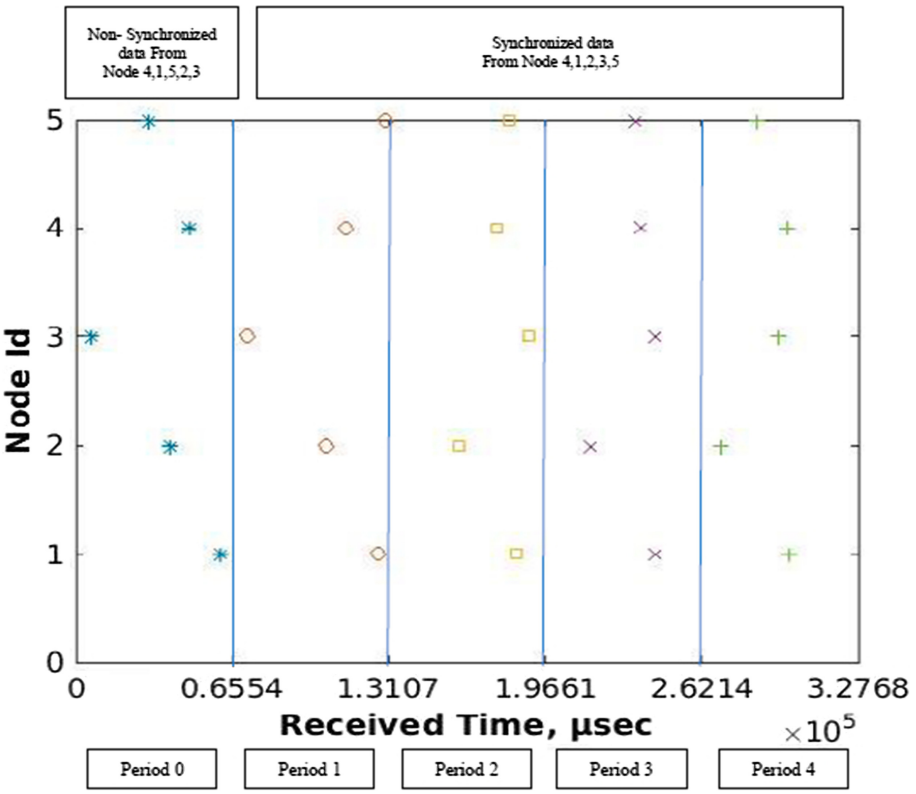

Fig. 6. The order of packet received by the basestation from 5 nodes using the dynamic data transmission scheduling for Synchronicity

5.2 Statistical Test on the Synchronization Period for 5 Nodes

Table 1 and Table 2 showed the results of the average synchronization period for the individual nodes for both experiment settings. These samples were taken for every 100th period of the data received at the basestation. While the *p-value* is

the statistical procedure of the *t-test* by taking the average synchronized period of every cycle of each individuals.

Table 1 shows that the synchronization period for every cycles of each individuals were stable. This also shows that the data were propagating between 31999.5 µs to 32319 µs. Whereas for Table 2 showed the average synchronization were inconsistent in every cycle of the individual nodes. This showed that the biosensors were still trying to propagate according to the firefly transmission algorithm.

While the *p-value* from the *t-test* showed that the average synchronized period fof the random time synchronization were consistent and statistically significant at 1.11×10^{-9}, however the dynamic time synchronization showed better results between 1.11×10^{-36} and 9.13×10^{-22}. This also shows that the dynamic time synchronization had higher probability for all the nodes transmitted and received by the basestation. With the consistency of the synchronization period means that the packets delivered and received by the basestation was in synchronized.

Table 1. Average of synchronization period of random time synchronization for 5 nodes.

Node ID	p-value	Average of synchronization period (μsec)				
		Cycle 1	Cycle 2	Cycle 3	Cycle 4	Cycle 5
Node 1	1.14×10^{-9}	31999.5	31998.4	32639.4	32318.2	32319
Node 2	1.14×10^{-9}	31999.5	31998.4	32639.4	32318.2	32319
Node 3	1.14×10^{-9}	31999.5	31998.4	32639.4	32318.2	32319
Node 4	1.14×10^{-9}	31999.5	31998.4	32639.4	32318.2	32319
Node 5	1.14×10^{-9}	31999.5	31998.4	32639.4	32318.2	32319

Table 2. Average of synchronization period of dynamic data transmission scheduling for 5 nodes.

Node ID	p-value	Average of synchronization period (μsec)				
		Cycle 1	Cycle 2	Cycle 3	Cycle 4	Cycle 5
Node 1	1.11×10^{-36}	55915.4	57157.4	56631.5	56036.1	56608.2
Node 2	3.72×10^{-24}	56653.4	49318.9	50668.3	47461.3	52049.4
Node 3	9.13×10^{-22}	51784.2	42139.4	50583.6	50047.2	53968.1
Node 4	1.27×10^{-22}	52591.8	53990.8	53285.6	46202	44065
Node 5	2.87×10^{-23}	47374.6	49972.9	47366.6	52741.6	47858.3

5.3 Sequencing of Packet Delivered for 10 Nodes

Figure 7 and Fig. 8 show the synchronization process of the ten (10) sensor nodes for random and dynamic time synchronization respectively. This shows that in the time synchronization approach will automatically synchronized, once it detected the node transmitting the data to the basestation. Even though the time took for all nodes to be in synchronized was very short, but there will always have a communication overhead which can lead to the node and communication link failure. By observation the communication process, during the initial rounds of the synchronization period only 20% the data transmitted in a synchronized pattern, then in a short period of time one or two sensor nodes rearrange the position. The rearrangement of the sensor nodes caused by the communication overhead, which leads to the delay in transmission of the sensor nodes.

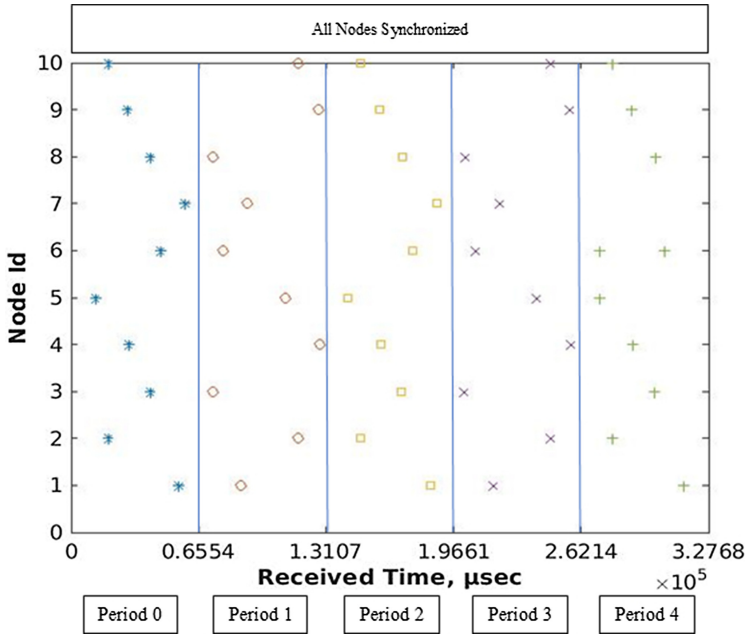

Fig. 7. The order of packet received by the basestation from 10 nodes transmitting at random

Figure 8 shows that the nodes were trying to synchronize the data, hence the unstable received time at the basestation. This basically shows that as the number of nodes increases, the more difficult for the algorithm to synchronize the data for the basestation. During the initial phase, period 0, Node 10 was not detected during the first cycle. While in Period 3, it was observed that Node 4 was not received by the basestation. The reason for Node 4 and Node 10 were not broadcasted, may cause by battery efficiency or unpredictable intermittence

connectivity of the sensor node. The unpredictable interference can cause the shift in the propagation time of the transmission. Since Node 4 was not received by the basestation to utilize the bandwidth of Period 3, Node 1 was broadcasted twice. This showed that since the sensor nodes were trying to adjust their phase time in the systems, only 20% of the time the data transmitted in a synchronized pattern. The remaining time, the sensor nodes were still trying to adjust their phase time.

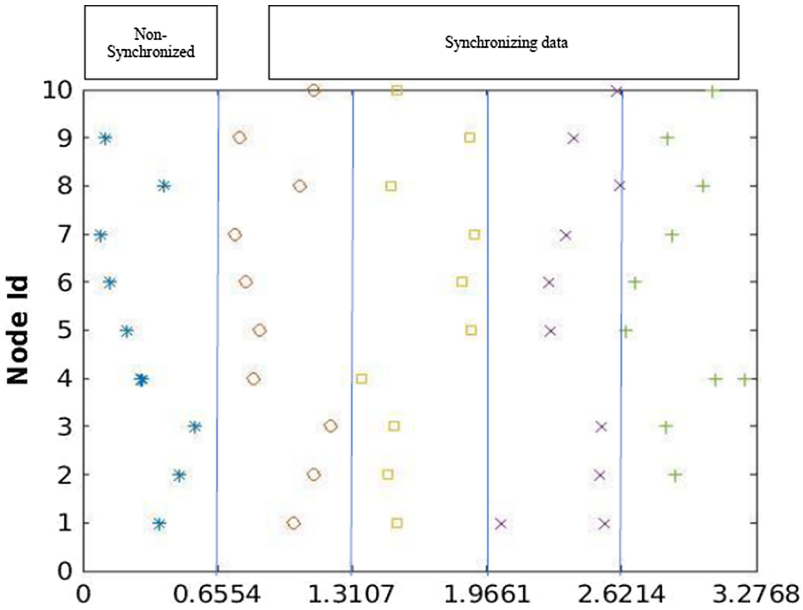

Fig. 8. The order of packet received by the basestation from 10 nodes using dynamic data transmission scheduling algorithm for Synchronicity

5.4 Statistical Test on the Synchronization Period for 10 Nodes

Table 3 shows the results obtained for the average synchronized period for every cycle of each individuals were consistent and statistically significant. This means that the individual nodes transmitted the packets at the same period throughout, this also shows that there was no delay during the transmission of the system.

From Table 4 shows the average synchronization period for every 100th period using dynamic approach. The average of synchronized period shows the average oscillator period was around 34000 to 35000 µs. The data can be seen below that the packet data cannot correctly local clock completely and more time will be needed for the data to converge synchronization. Hence, the inconsistent in the average synchronization period. While the *p-value* shows that the probability of the sensor nodes to get synchronized was very high, between 6.80×10^{-18} and 4.63×10^{-24}.

Table 3. Average of synchronization period of random time synchronization for 10 Nodes.

Node ID	p-value	Average of synchronization period (μsec)				
		Cycle 1	Cycle 2	Cycle 3	Cycle 4	Cycle 5
Node 1	9.35×10^{-11}	31999	31998.6	31999.2	32318.2	32001.7
Node 2	9.35×10^{-11}	31999	31998.6	31999.2	32318.2	32001.7
Node 3	9.35×10^{-11}	31999	31998.6	31999.2	32318.2	32001.7
Node 4	9.35×10^{-11}	31999	31998.6	31999.2	32318.2	32001.7
Node 5	9.35×10^{-11}	31999	31998.6	31999.2	32318.2	32001.7
Node 6	9.35×10^{-11}	31999	31998.6	31999.2	32318.2	32001.7
Node 7	9.35×10^{-11}	31999	31998.6	31999.2	32318.2	32001.7
Node 8	9.35×10^{-11}	31999	31998.6	31999.2	32318.2	32001.7
Node 9	9.35×10^{-11}	31999	31998.6	31999.2	32318.2	32001.7
Node 10	9.35×10^{-11}	31999	31998.6	31999.2	32318.2	32001.7

Table 4. Average of synchronization period of dynamic data transmission scheduling for 10 Nodes.

Node ID	p-value	Average of synchronization period (μsec)				
		Cycle 1	Cycle 2	Cycle 3	Cycle 4	Cycle 5
Node 1	8.96×10^{-22}	31329.6	26203.5	25801.9	24545.9	27819.6
Node 2	1.12×10^{-22}	35628	35089	34357.3	33266.3	32946.8
Node 3	1.12×10^{-22}	35628	35089	34357.3	33266.3	32946.8
Node 4	1.12×10^{-22}	35628	35089	34357.3	33266.3	32946.8
Node 5	8.89×10^{-22}	31790.9	34183.8	33331.5	34163.6	32969.5
Node 6	7.82×10^{-22}	34719.3	33453.7	33574.7	34102.3	33613.5
Node 7	6.80×10^{-18}	32963.8	32490.8	33815.2	34471.3	38389
Node 8	4.63×10^{-24}	34015.4	34102.5	33598.5	33540.8	34166.5
Node 9	1.55×10^{-21}	34710.1	33250	32960.4	33042.3	32708.3
Node 10	2.39×10^{-19}	35226.8	36789.5	32684.9	31922.1	33407.9

5.5 Sequencing of Packet Delivered for 15 Nodes

In the synchronization process for 15 nodes, the results shown in Fig. 9 and Fig. 10 were for random and dynamic time synchronization respectively. Figure 9 result observed that 45% of the nodes were in synchronized manner. It was also observed that at a certain period the nodes, one of the node was not transmitted and caused the nodes shifted their time of transmission. Once all of the nodes shifted, 20% of the nodes transmitted were synchronized. The reason for the delay in transmission was because there was a delay in transmission of the packets. The reason of the delay can be because of the position of the two sensor

nodes, will be the position of sensor nodes either Even though the nodes were in synchronized patterns, the nodes' time shown there were drifted which caused the communication overhead high.

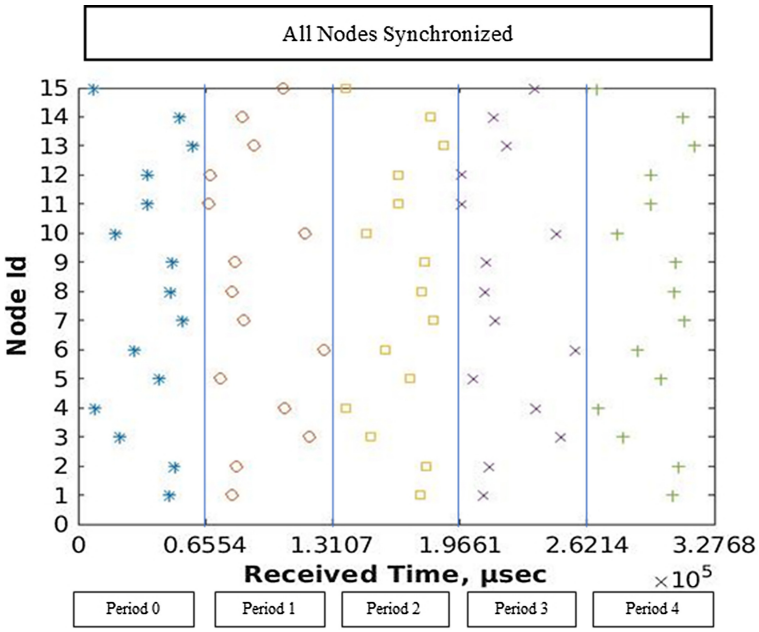

Fig. 9. The order of packet received by the basestation from 15 nodes transmitting at random

Figure 10 shows the synchronization process of the 15 sensor nodes was similar with 10 nodes, where the synchronization process took very long to synchronize the data. It shows that in every period, some of the nodes were transmitted twice in the same cycle. This means that there was a delay in transmitting form one of the biosensors, hence the repeat of biosensor received at the basestation to utilize the bandwidth. The result shows that the sensor nodes in Period 3 and Period 4, the basestation received the data were equally divided within the bandwidth time slot. By observing the results, only 10% of the time the basestation able to receive the data in synchronicity manner. However, it still showed that one or two nodes packets drop or delay in the transmission to the basestation.

5.6 Statistical Test on the Synchronization Period for 15 Nodes

In the next set of the result will be the average synchronization period of the fifteen (15) nodes as shown in Table 5 and Table 6 for random and dynamic time synchronization respectively. Both Tables show that the average synchronization period for each individual nodes were inconsistent, however the random

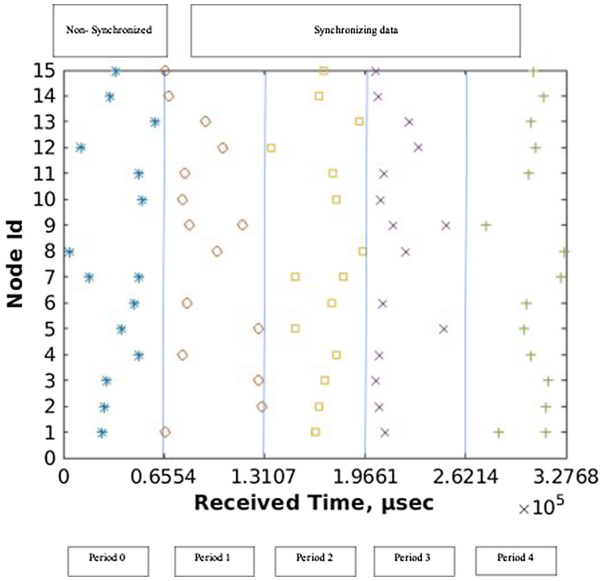

Fig. 10. The order of packet received by the basestation from 5 nodes using the firefly transmission scheduling algorithm for Synchronicity

time synchronization the average synchronization period were between 31997 and 32959.5 µs. This shows that the sensor nodes were propagating along the oscillator clock.

Table 6 below shows that as the number of sensor increases, the average synchronization period for all cycles becomes inconsistent and unstable. The timing of transmission by individual sensor node is different at every cycle which caused the delay by the clock drift. The drift is usually small, but it can be accumulated and compensated to cause message delay or packet loss.

5.7 Evaluation of Packet Delivery Rate

Figure 11 and Fig. 12 below shows the calculated packet delivery ratio (PDR) of the two(2) synchronization algorithms for 5, 10 and 15 sensor nodes. PDR is a ratio of the number of packets received by the basestation to the total number of sensor nodes send to the basestation. The result have shown that the PDR of the random time synchronization was ranges from 98% to 100%, while in the dynamic time synchronization the PDR was between 65% to 100%. This shows that the dynamic time synchronization, the PDR become more unstable as the number of biosensors increases. This also shows that the one or more biosensors will be lost when the system becomes larger.

Table 7 and Table 8 below show the results of the average packet delivery rate for every 100 synchronization rounds. In theory, the value of PDR will be decreased as the number of nodes increased. In the random time synchronization

Table 5. Average of synchronization period of random time synchronization for 15 Nodes.

Node ID	p-value	Average of synchronization period (μsec)		
		Cycle 1	Cycle 2	Cycle 3
Node 1	1.09×10^{-5}	32318.4	31999.8	32318.7
Node 2	7.40×10^{-5}	32637.3	32321	33278.7
Node 3	4.15×10^{-10}	31998.7	32000.1	31997.8
Node 4	1.10×10^{-5}	32318.1	31998.5	31999.6
Node 5	1.15×10^{-9}	31999.3	31996.1	31999.5
Node 6	5.16×10^{-10}	31998.8	32000.9	31998.7
Node 7	1.01×10^{-9}	31997.6	31997	32000.3
Node 8	1.54×10^{-5}	31999.9	31998.3	32000.3
Node 9	7.12×10^{-10}	32000.1	31997.7	32000.4
Node 10	1.10×10^{-5}	32318.2	31998.4	32000.3
Node 11	1.12×10^{-5}	32320.6	31996.1	31999.5
Node 12	4.30×10^{-5}	32318.1	32320.7	32959.5
Node 13	1.53×10^{-9}	31997	31997.8	32001.1
Node 14	2.08×10^{-9}	32001.5	31996.5	31999.7
Node 15	1.50×10^{-9}	31998.1	31997.8	32001.6

Table 6. Average of synchronization period of dynamic data transmission scheduling for 15 Nodes.

Node ID	p-value	Average of synchronization period (μsec)				
		Cycle 1	Cycle 2	Cycle 3	Cycle 4	Cycle 5
Node 1	1.10×10^{-74}	34929.1	32720.9	32689.9	30173.8	33561.9
Node 2	8.44×10^{-82}	38084.9	32870	39859	30647.9	36678.5
Node 3	8.44×10^{-82}	38084.9	32870	39859	30647.9	36678.5
Node 4	8.44×10^{-82}	38084.9	32870	39859	30647.9	36678.5
Node 5	4.57×10^{-86}	29345.3	31797.1	32822.7	33378.1	31611.6
Node 6	1.38×10^{-78}	32981	33050.5	36105.5	35942.5	35517.1
Node 7	1.44×10^{-76}	34558.5	33487	29396.7	32915.3	34461.8
Node 8	7.14×10^{-85}	31981.5	35921.7	32704.8	36109.3	33359.9
Node 9	4.59×10^{-83}	33857.8	35771.4	39013.1	33226.5	31681.6
Node 10	1.96×10^{-78}	29992.7	35813.4	32648.8	37520.6	40158.4
Node 11	2.76×10^{-84}	28539.1	35680.4	32546.6	39652.6	34894.1
Node 12	1.88×10^{-82}	29903.1	35824	32494.9	35365.3	39124.3
Node 13	3.32×10^{-78}	32695.9	39662.8	35504.2	29055.1	33221.2
Node 14	3.32×10^{-78}	32695.9	39662.8	35504.2	29055.1	33221.2
Node 15	3.32×10^{-78}	32695.9	39662.8	35504.2	29055.1	33221.2

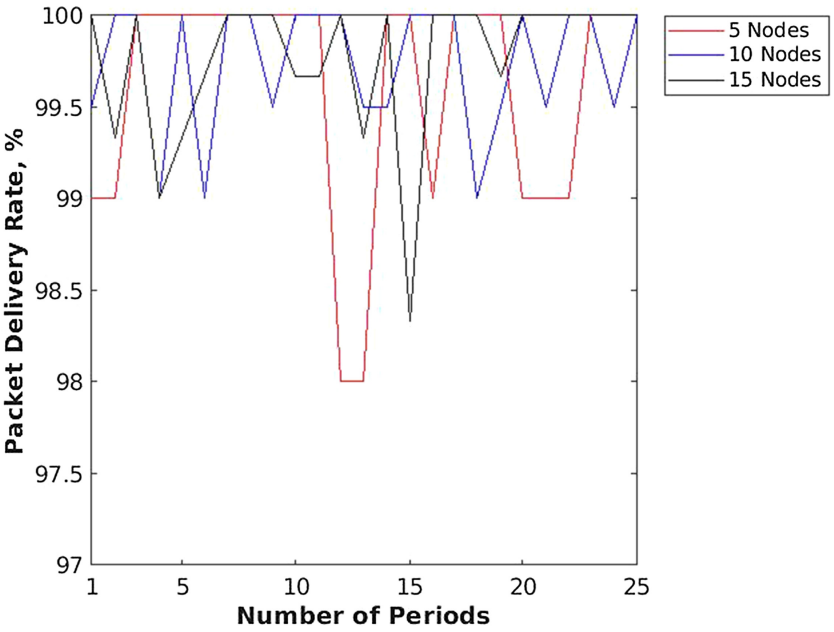

Fig. 11. The Packet Delivery Rate for 5, 10, 15 nodes transmitting at random time synchronization

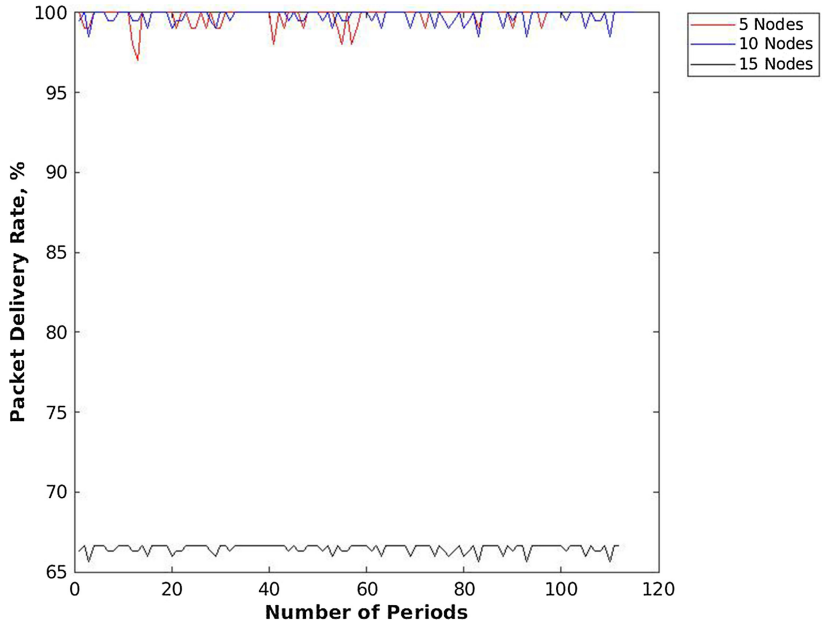

Fig. 12. The Packet Delivery Rate for 5, 10, 15 nodes using the dynamic data transmission scheduling algorithm for Synchronicity

algorithm as shown in Table 7, it shows that when the number of nodes was 5 the average PDR was 99.6% compared with number of nodes of 15 the average was 99.79%. In Period 3, the PDR of 5 nodes shows 99.2%, one of the reasons will be one or more nodes have low energy efficiency, hence loss of data during the transmission. This is caused by retransmitted packet due to collision as the numbers of nodes increases. From the graph also shows that as the number of nodes increases, the numbers of packets decreases during the transmission. This means that some of the packets sent by the sensor did not reach or received by the basestation. This mainly because there were traffic or congestions during the transmissions of the data.

Table 7. Average of Packet Delivery Rate (PDR) for 100 cycles using Random Time Synchronization for 5, 10, and 15 Nodes.

No of Nodes	p-value	Packet deliver rate %					
		Ave	P1	P2	P3	P4	P5
5	1.56×10^{-11}	99.6	99.6	100	99.2	99.6	99.6
10	2.81×10^{-11}	99.74	99.7	99.7	99.8	99.7	99.8
15	1.65×10^{-17}	99.79	99.53	99.87	99.47	99.93	100

Table 8 the result shows that has a better PDR compared to the time synchronization for 5 and 10 sensor nodes between 98% to 100%. However, when the sensor nodes were 15 the PDR of adaptive transmission scheduling was 66.5%. This means that some of the packets sent by the sensor did not reach or received by the basestation. This mainly because there were traffic or congestions during the transmissions of the data. The results show that the allocated time slots for the sensor nodes broadcast were very small for a large scalability. The transmission will be continuously and fast, thus will cause one or more sensor nodes were delay in transmission of the data.

Table 8. Average of Packet Delivery Rate (PDR) for 100 cycles using dynamic data transmission scheduling for 5, 10, and 15 Nodes.

No of Nodes	p-value	Packet deliver rate %					
		Ave	P1	P2	P3	P4	P5
5	1.62×10^{-222}	99.71	100	99	99	100	100
10	1.03×10^{-274}	99.75	99.5	100	98.5	100	100
15	3.93×10^{-267}	66.5	66.33	66.67	65.67	66.67	66.67

6 Discussion

In the random time synchronization, the results shows the packet delivery ratio was in the range of 99.20% to 100%. This PDR results were similar with the PDR in the simulation analysis; where the PDR were ranged between 90% to 100%. This shows that designing a network with random time synchronization can be done using the simulation tools. However, the simulation tools cannot implement the dynamic time synchronizaton scheduling approach.

In comparison of the performance between the time synchronization and the adaptive transmission scheduling approach. It shows that the adaptive transmission scheduling was better than time synchronization, in terms of synchronization pattern and utilizing the time slot of the sensor nodes. This type of synchronization proved that the sensor nodes broadcasted in a synchronized periodic manner and it proved that the behavior followed the mathematical model of Eq. 1. This also proved by using the *t- test*, it shows that the adaptive transmission scheduling has higher probability that the nodes able to broadcast the data to the basestation.

In the random time synchronization approach the testbeds show that the synchronization period was better than the adaptive transmission scheduling. This mainly because the random time synchronization nodes will only consider the previous firing nodes and repeat the cycle. While in the adaptive transmission scheduling approach the result shows that nodes were able to transmit the data in a synchronize pattern and utilize the bandwidth. However, this approach will do better in a smaller scale compared to large scale of WBAN. As mentioned in Dressler et al. [5], network with a large scale of wireless communications can exceed the capacity and leads to low reliability due to the packet loss. The loss of packets can be also due to transmission collision, because of the concurrent transmission of the sensor nodes. Hence, the packet delivery rate of the dynamic time transmission synchronization were between 66.5% and 99.71% as shown in Fig. 12 and Table 8.

7 Conclusion

From the results, although the dynamic data transmission synchronization using the firefly algorithm. The results showed that the algorithm can reduce the energy consumption with longer sleeping period, however it is not able to maintain the PDR when the number of nodes increases. In order to improve the PDR, the firefly algorithm needs to be enhanced as a future work. The process of this approach is to have the time of the transmitted data in a decentralized synchronization protocol. The application of this protocol is to have the reliable and accurate distribution of synchronization procedures.

References

1. Ramlall, R.: Wireless Body Area Network Time Synchronization using R Peak Reference Broadcasts (2007)
2. Yildrim, K., Gurcan, O.: Efficient time synchronization in a wireless sensor network by adaptive value tracking. IEEE Trans. Wireless Commun. **13**(7), 3650–3664 (2014)
3. Wu, T.Y., Wang, W.: An improvement mechanism for heartbeat-driven MAC synchronization in wireless body sensor network. Int. J. Commun. Syst. **33**(4), e4224 (2019)
4. Werner-Allen, G., Tewari, G., Welsh, M., Nagpal, R.: Firefly- inspired sensor network synchronicity with realistic radio effects. In: Sensys (2005)
5. Dressler, F., Akan, O.: A survey of bio-inspired approach networking. Comput. Netw. **54**(6), 81–900 (2010)
6. Lee, C.J., Jung, J.Y., Lee, J.R.: Bio-inspired distributed transmission power control considering QoS fairness in wireless body area sensor networks. Sens. J. **17**(10), 2344 (2017)
7. Mirollo, R., Strogatz, S.: Synchronization of pulse-coupled biological oscillator. SIAM J. Appl. Math. **50**(6), 1645–1662 (1990)
8. An, Z., Zhu, H., Zhang, M., Xu, C., Xu, Y., Li, X.: Linear pulse- coupled oscillators model- a new approach for time synchronization in wireless sensor networks. Sci. Res. J. **2**, 108–114 (2010)
9. Adhikary, S., Chattopadhyay, S., Choudhury, S.: A Novel bio-inspired algorithm for increasing throughput in wireless body area network (WBAN) by mitigating inter-wban interference. In: Chaki, R., Cortesi, A., Saeed, K., Chaki, N. (eds.) Advanced Computing and Systems for Security. AISC, vol. 667, pp. 21–37. Springer, Singapore (2018). https://doi.org/10.1007/978-981-10-8183-5_2